(IJIEEE) 2026, Vol. No. 12, Issue 1, Jan-Dec **e-ISSN: 2454-9592; p-ISSN: 2454-8081**

Design of Voltage Mode Control for Multi-Output Flyback Converter

***Sanjana S M, **Dr Arpitha Raju B**
*Postgraduate, **Professor
Dr. Ambedkar Institute of Technology, Bengaluru

[1]*Received: 21/11/2025; Accepted: 22/12/2025; Published: 13/01/2026*

Abstract

Voltage regulation employing a fixed-frequency control strategy is implemented for flyback converters utilizing the DCM (discontinuous conduction mode). The regulation variables are formulated to maintain the converter's operation extent feasible to the boundary of transition mode, thereby establishing a systematic design methodology for the flyback converter. While this method is appropriate to any converter carrying out in DCM, the primary focus of this study is the flyback topology. The multi-output flyback converter is designed to deliver low-voltage, low-current outputs with minimal ripple. The proposed converter handles a modulating frequency of 100 kHz. Post-regulation at the secondary side is implemented using low-dropout regulators to enhance line regulation, load regulation, and cross-regulation performance.

Introduction

Switched-mode power supplies have gained widespread adoption on account of their optimal performance, elevated power flow intensity, and lower cost relative to linear power supplies. This topology is particularly well-suited for remote, cost-sensitive energy source applications, as it provides input-output isolation while requiring fewer semiconductor and magnetic elements over alternative SMPS configurations. Flyback converters can drive in three approaches: CCM, DCM and CrCM, the latter representing the transition between the other two modes. CrCM offers notable advantages over CCM, ZCS of the switch and ZVS of the freewheeling diode, thereby reducing switching losses and mitigating electromagnetic interference. The current stress in CrCM is higher than in CCM but lower than in DCM. Furthermore, feedback compensation is simplified in CrCM since the flyback converter exhibits a first-order transfer function under these operating conditions. Despite these benefits, the primary limitation of CrCM is the variable switching frequency that arises in response to changes in output load. This study proposes a voltage regulation strategy based on a constant-frequency mechanism, which modulates the load voltage according to the occurrence of variation in gate pulses to operate the flyback converter in the CrCM (critical conduction mode). The recommended control approach is simple, cost-effective, and resilient to converter setting changes, and it provides a superior dynamic response. Because it combines the inherent benefits of isolated converters with lower complexity and cost compared to traditional isolated topologies, the proposed converter is especially well-suited for low-power, multi-output implementation.

Proposed Multi Output Flyback Converter

The structure of proposed converter is shown below.

[1] [1] *How to cite the article:* Sanjana S.M., Arpitha R.B.; Design of Voltage Mode Control for Multi-Output Flyback Converter; *International Journal of Inventions in Electronics and Electrical Engineering*, 2026, Vol 12, 8-16

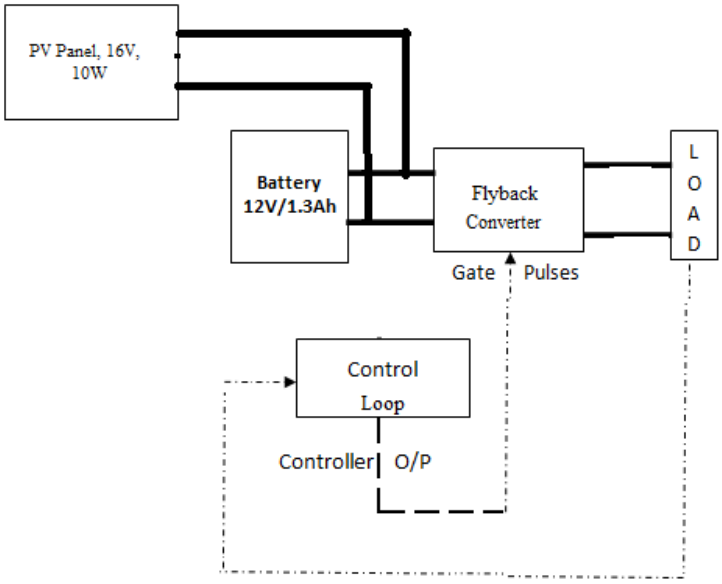

The high-frequency transformer's primary and secondary windings function as two magnetically connected inductors. Energy is accumulated in the primary winding during the ON-state of the MOSFET and is subsequently transferred to the secondary winding during the OFF-state. The converter operates in three distinct modes: CrCM, CCM and DCM.

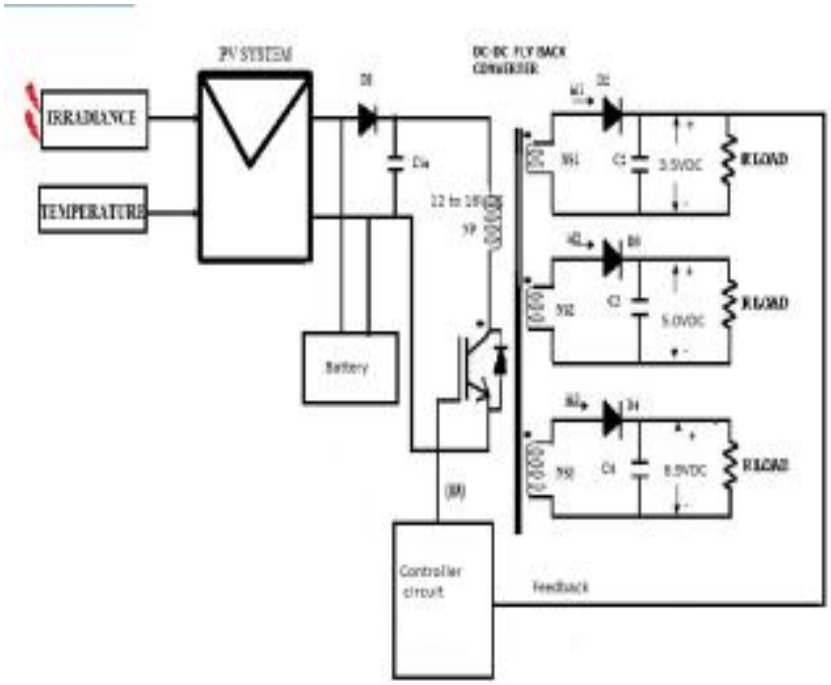

It is not until the second ON cycle begins that the flyback transformer's energy is fully delivered to the load in CCM.On the other hand, In discontinuous conduction mode, the load receives the entirety of the stored energy during the OFF cycle. The critical conduction mode, also referred to as the transition mode, occurs at the limits between DCM and CCM. The high-frequency transformer provides electrical isolation and power transfer while maintaining balance between the source and load sides of the circuit. Rectifying diodes (D_1, D_2, D_3) and capacitors (C_1, C_2, C_3) constitute essential components of the flyback converter's secondary stage, facilitating voltage rectification and filtering. Moreover, the converter's feedback control system adjusts the MOSFET duty cycle to regulate and retain the desired load voltage.

FLYBACK CONVERTER

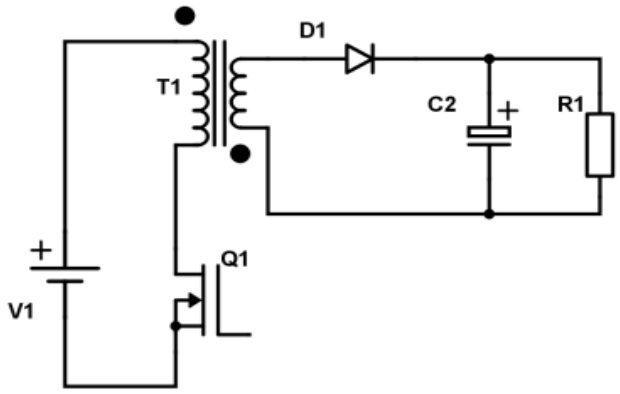

In a buck-boost converter topology, the inductance is substituted by a transformer to realize a flyback converter. The gain of the flyback converter can be illustrated as given below

$$\frac{V_{out}}{V_{in}} = \frac{N_2}{N_1} * \frac{D}{1-D}$$

:

$N1$: The total quantity of turns present on transformer's primary side

$N2$: The total quantity of turns present on transformer's secondary side.

The gain of the flyback converter can be derived by evaluating the two states of the power electronic switch (Q_1), in a manner analogous to the buck-boost converter. When Q_1 is turned ON, the source voltage is solicited across the transformer's primary side, effectuating the energy to be accumulated in the magnetizing inductance LmL_mLm. Due to the dot convention shown in Figure 1, diode D_1 remains reverse-biased, and a negative voltage appears across it. In the mean time, the load current is supplied by the output capacitor C1C_1C1. When Q_1 is turned OFF, the current in LmL_mLm cannot instantaneously drop to zero; consequently, energy is transferred from the magnetizing inductance to the output capacitor C1C_1C1 as diode D_1 becomes forward-biased, consistent with Faraday's law of electromagnetic induction. Figure 2 illustrates the voltage and current waveforms corresponding to the ON and OFF states of Q_1, where IpI_pIp denotes the peak current in the transformer. 's primary side (T1).

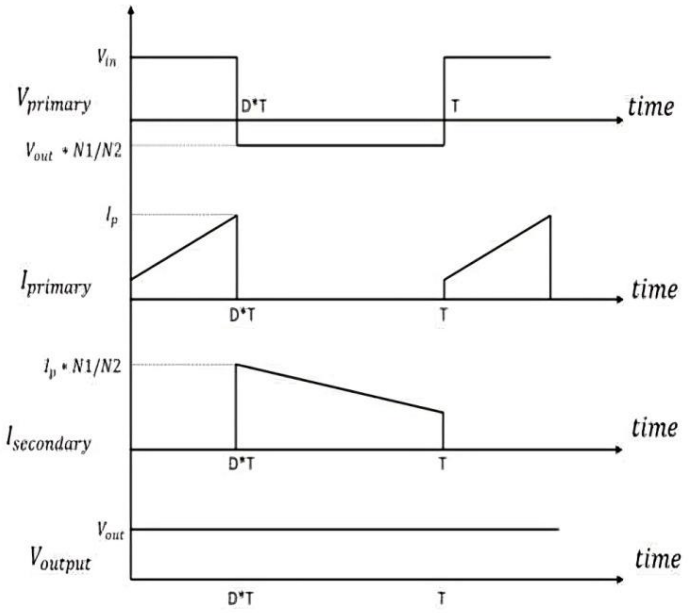

The voltage and corresponding gain expression can be acquired by relating the average voltage principle to the primary winding of the transformer (T_1).

$$V_{in} * D * T - V_{out} * \frac{N_1}{N_2} * (1 - D) * T = 0$$

$$\Rightarrow \frac{V_{out}}{V_{in}} = \frac{N_2}{N_1} * \frac{D}{1 - D}$$

SIMULATION SETUP & RESULTS

The values of the parameters utilized in the simulation are displayed below in Table I:

TABLE-I SIMULATION PARAMETERS

Parameters	**Values**
Load Voltage (in volts)	3.3 V, 5V, 6.7V
Load Power (in watts)	15W
Switching Frequency	100 KHz
PV Voltage	13V
Battery voltage	12V
Battery Capacity	7.5Ah

The simulation circuit for proposed converter is provided below:

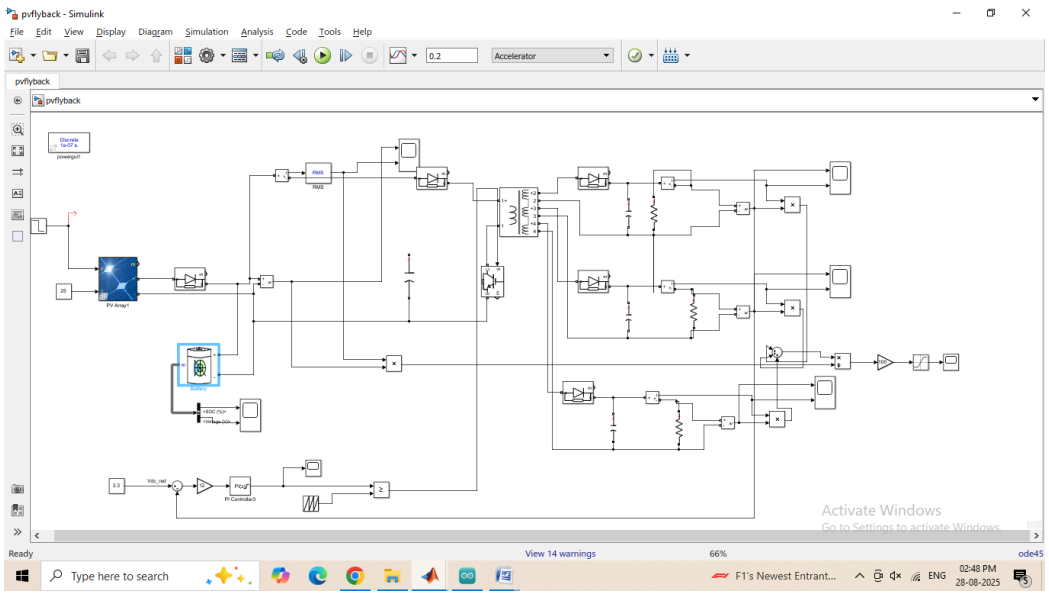

This involves supplying the flyback converter with multiple rectified outputs with a 13V PV voltage in order to deliver loads. Here, the PV irradiation is adjusted based on the table that follows:

Time(s)	0	0.05
Irradiance(W/m2)	1000	300

The PV voltage and current is provided below:

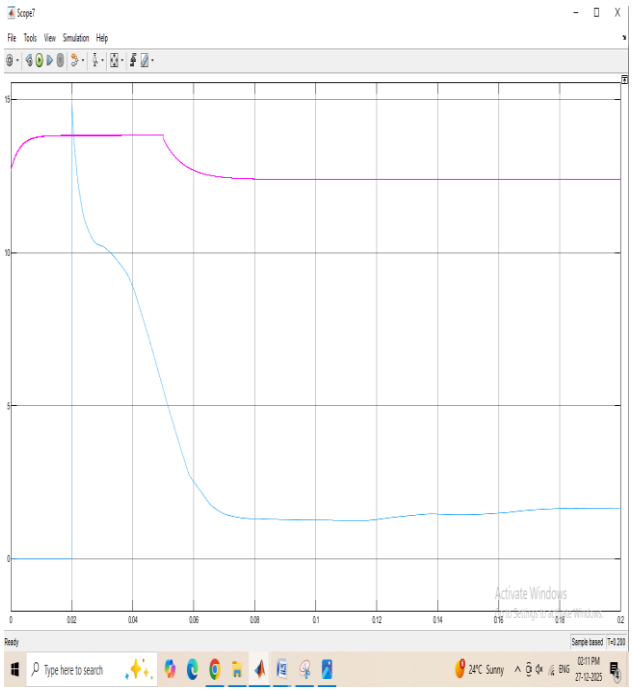

For 1000W/m2 of irradiance, the PV voltage and current are around 13V and 1.7A, respectively. As the irradiance is decreased, the PV voltage and current also decrease. The duty ratio produced by the PI controller is given below, and the PI control-based voltage control loop is utilized to keep a regulated output voltage:

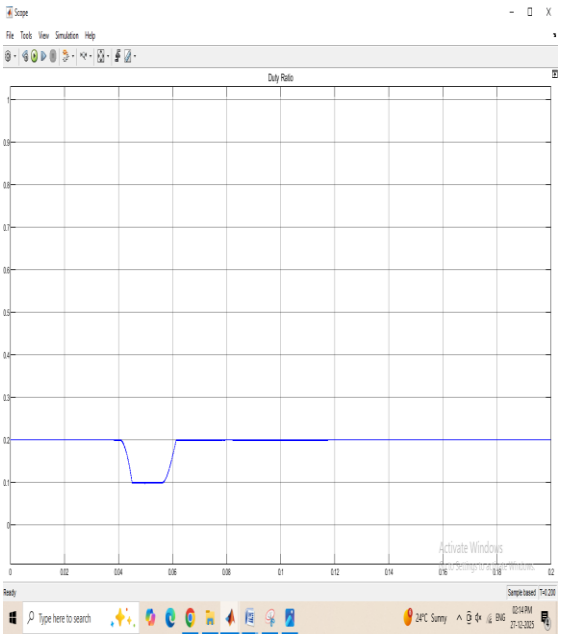

The figures above illustrate how duty ratios vary for regulated loads (ranging from 0.1 to 0.2). Below are the battery's voltage and percentage SOC:

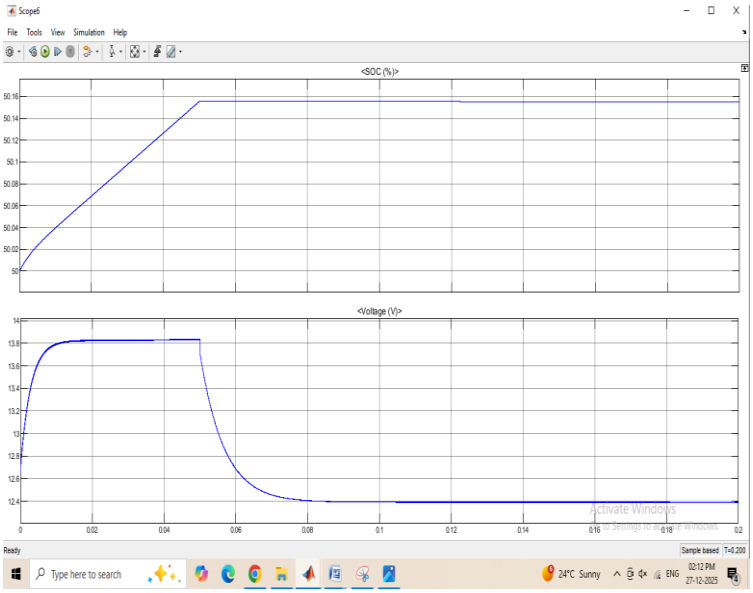

When a PV source is available, the battery is initially charging and its state of charge (SOC) rises; when the PV source is unavailable, the battery begins to drain and its SOC falls. Below are the load voltage and current:

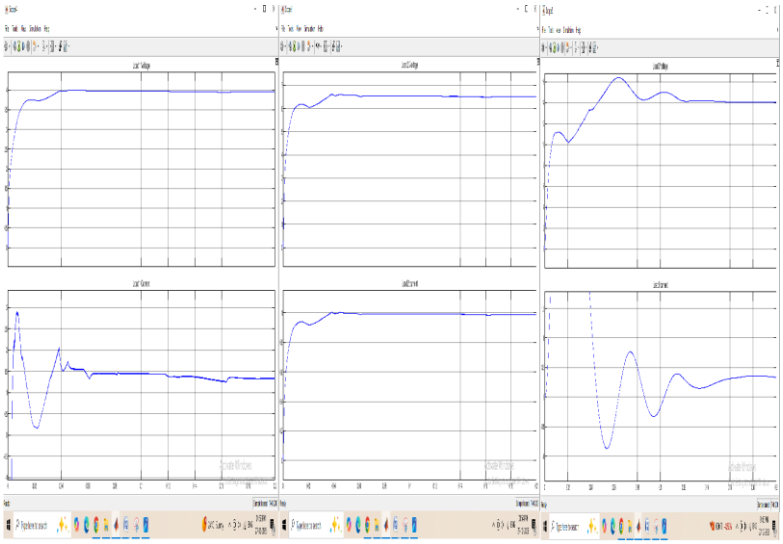

When the irradiance is reduced, the battery is used to regulate the voltage. For a 6.6W load, the voltage is approximately 6.6V and the current is 1A; for a 12W load, the voltage is approximately 14V and the current is 0.8A; and for a 4W load, the voltage is 4V and the current is 1A. The converter's efficiency is shown below:

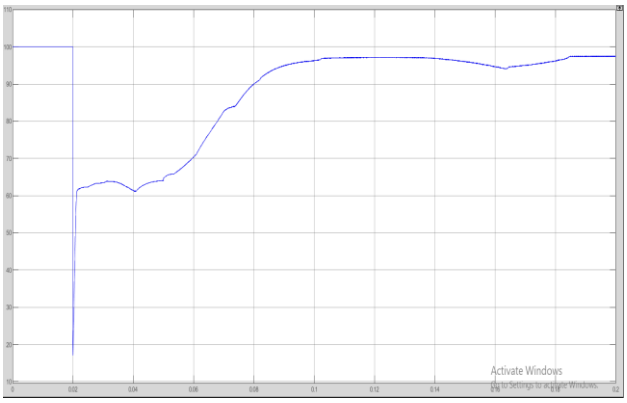

Approximately 97.4% of the converter is efficient. The loads have been switched to R, RC (battery), and RL (DC motor) loads. The motor speed for the RL load and the percentage SOC for the RC load are given below:

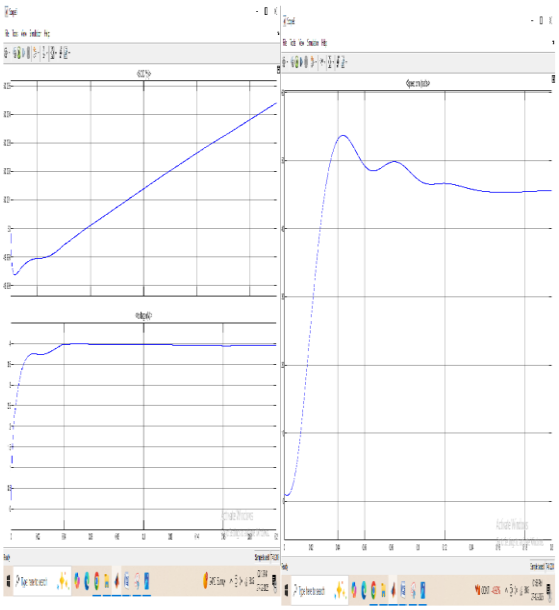

The motor is operating at 45 rad/s while the load battery is charging for both the PV source and the battery source. The overall efficiency of the recommended converter with R, RC, and RL loads is displayed below:

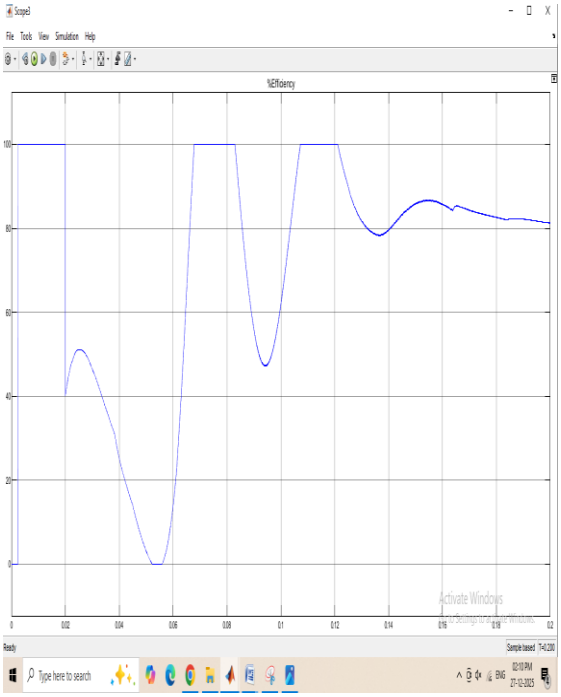

When the loads are switched to R, RC (battery), and RL (DC motor) loads, the efficiency of the suggested converter is approximately 80%.

CONCLUSION

In this, the multi output flyback converter is designed and simulated with various types of load with varying irradiation for PV source. The voltage mode control is designed for single load and thereby controls other loads too in varying input conditions. The efficiency of the converter is 97.4% with resistive loads.

REFERENCES

Chang, C., He, L., Bian, B., & Han, X. (2019). Design of a highly accurate PSR CV/CC AC-DC converter based on a cable compensation scheme without an external capacitor. *IEEE Transactions on Power Electronics, 34*(10), 9552–9561. https://doi.org/10.1109/TPEL.2019.2890448

Chen, M. G., Xu, S., Huang, L., Sun, W., & Shi, L. (2021). A novel digital control method of primary-side regulated flyback with active clamping technique. *IEEE Transactions on Circuits and Systems I: Regular Papers, 68*(2), 950–962. https://doi.org/10.1109/TCSI.2020.3037481

Li, Y., & Zhu, Z. (2020a). A constant current control scheme for primary-side controlled flyback controller operating in DCM and CCM. *IEEE Transactions on Power Electronics, 35*(9), 9464–9472. https://doi.org/10.1109/TPEL.2019.2954616

Li, Y., & Zhu, Z. (2020b). A capacitor-free control scheme for a primary-side controlled flyback converter. *IEEE Transactions on Power Electronics, 35*(9), 9484–9495. https://doi.org/10.1109/TPEL.2019.2954532

Patnaik, L., Praneeth, A. V. J. S., & Williamson, S. S. (2019). A closed-loop constant-temperature constant-voltage charging technique to reduce charge time of lithium-ion batteries. *IEEE Transactions on Industrial Electronics, 66*(2), 1059–1067. https://doi.org/10.1109/TIE.2018.2868118

Tang, T. Y., Luo, P., Deng, C., & Zhang, B. (2021). Seamless mode-switch control scheme for primary side regulation flyback with capacitorless self-adaptive startup. *IEEE Transactions on Power Electronics, 36*(8), 9668–9677. https://doi.org/10.1109/TPEL.2020.3048271

Wi, S.-M., Lee, J. S., & Kim, M. (2018). Exponentially stable Lyapunov-function-based controller for a flyback CCM converter. *IEEE Transactions on Industrial Electronics, 65*(2), 1213–1225. https://doi.org/10.1109/TIE.2017.2757260

Wu, Q., & Zhu, Z. (2017). A versatile OCP control scheme for discontinuous conduction mode flyback AC/DC converters. *IEEE Transactions on Industrial Electronics, 64*(8), 6443–6452. https://doi.org/10.1109/TIE.2017.2657019

Wu, W.-C., Liang, T.-J., Chen, K.-H., & Li, C.-Y. (2018, April). Quasi-resonant flyback converter with new valley voltage detection mechanism. In *Proceedings of the IEEE Applied Power Electronics Conference and Exposition* (pp. 767–770). https://doi.org/10.1109/APEC.2018.8341318

Zhu, Z., Wu, Q., & Wang, Z. (2017). Self-compensating OCP control scheme for primary-side controlled flyback AC/DC converters. *IEEE Transactions on Power Electronics, 32*(5), 3673–3682. https://doi.org/10.1109/TPEL.2016.2622644